AAPS PharmSciTech (2022) 23: 88
DOI: 10.1208/s12249-022-02240-w

Research Article

Theme: Advancements in Modified-release Oral Drug Delivery - Delivery throughout the Gastro-intestinal Tract

Anti-oxidant Containing Nanostructured Lipid Carriers of Ritonavir: Development, Optimization, and *In Vitro* and *In Vivo* Evaluations

Srinivas Reddy Jitta,[1] Navya Ajitkumar Bhaskaran,[1] Salwa,[1] and Lalit Kumar[1,2]

Received 9 January 2022; accepted 20 February 2022; published online 16 March 2022

Abstract. Acquired immunodeficiency syndrome (AIDS) is a condition caused by the infection of a retrovirus namely, human immunodeficiency virus (HIV). Currently, highly active anti-retroviral therapy (HAART), a combination of anti-viral drugs belonging to different classes is considered to be effective in the management of HIV. Ritonavir, a protease inhibitor (PI), is one of the most important components of the HAART regimen. Because of its lower bioavailability and severe side effects, presently, ritonavir is not being used as a PI. However, this drug is being used as a pharmacokinetic boosting agent for other PIs such as lopinavir and in lower doses. The current study aimed to develop nanostructured lipid carriers (NLCs) encapsulating ritonavir to reduce its side effects and enhance oral bioavailability. Ritonavir-loaded NLCs were developed using a combination of two different solid lipids and liquid lipids. Alpha-tocopherol, a well-known anti-oxidant, was used as an excipient (liquid lipid) in the development of NLCs which were prepared using a simple hot-emulsion and ultrasonication method. Drug-excipient studies were performed using Fourier transform infrared spectroscopy (FTIR) and differential scanning calorimetry (DSC). QbD approach was followed for the screening and optimization of different variables. The developed NLCs were characterized for their particle size (PS), polydispersity index (PDI), zeta potential (ZP), and entrapment efficiency (EE). Furthermore, NLCs were studied for their *in vitro* drug release profile, and finally, pharmacokinetic parameters were determined using *in vivo* pharmacokinetic studies. The optimized NLC size was in the range of 273.9 to 458.7 nm, PDI of 0.314 to 0.480, ZP of −52.2 to − 40.9 mV, and EE in the range of 47.37 to 74.51%. From *in vitro* drug release, it was found that the release of drug in acidic medium was higher than phosphate buffer pH 6.8. Finally, *in vivo* pharmacokinetic studies revealed a 7-fold enhancement in the area under the curve (AUC) and more than 10-fold higher C_{max} with the optimized formulation in comparison to pure drug suspension.

KEY WORDS: ritonavir; nanostructured lipid carriers; alpha-tocopherol; HIV; pharmacokinetics.

INTRODUCTION

HIV infection has become one of the most serious healthcare issues for the mankind across the globe over the past few decades. Later stages of HIV infection damage the immune system to a great extent, and the condition is called as AIDS (1). According to WHO statistics, approximately 36 million people lost their lives so far because of HIV infection, and 1.5 million people are newly infected in the year 2020 (2). Currently, FDA approved more than 25 drugs under various classes for HIV treatment (3). A combination of drugs belonging to three or four different classes known to be effective in HIV treatment is considered as HAART (4). Despite the conflicting reports over HAART therapy, it has been accepted as the mainstay of medicines for HIV treatment (5).

Ritonavir is a protease inhibitor that was approved by US FDA in the year 1996 for use alone or in combination with other PIs in patients with advanced HIV infection (6). Molecular formula of ritonavir is $C_{37}H_{48}N_6O_5S_2$ (720.9 g/mol) (7). It is a lipophilic molecule, and because of its poor water solubility and high permeability, ritonavir is categorized as a BCS class II drug (8, 9). The intestinal permeability of ritonavir is low to moderate, and it is a substrate of P-glycoprotein (P-gp) with a moderate to high efflux ratio (6). It plays a key role in controlling cellular efflux of other PIs

[1] Department of Pharmaceutics, Manipal College of Pharmaceutical Sciences, Manipal Academy of Higher Education (MAHE), Manipal, Udupi, Karnataka 576 104, India.
[2] To whom correspondence should be addressed. (e–mail: lk.kundlas@gmail.com; lalit.kumar@manipal.edu)

1530-9932/22/0400-0001/0

through P-gp and the multidrug resistance–related protein 1 (MRP-1) efflux channels because of its ability to inhibit CYP3A4 isoenzyme of cytochrome P450 present in the liver and gastrointestinal tract. This results in lowering the metabolism of co-administered PIs and change in their pharmacokinetic parameters like half-life ($t_{1/2}$), maximum concentration (C_{max}), and AUC. Hence, ritonavir is being used as a boosting agent for other PIs in combination therapy to raise the bioavailability of co-administered drugs (10).

In the recent past, many researchers made attempts in the development of novel formulations of ritonavir to improve its oral bioavailability. These formulations include pro-liposomes (11), solid lipid nanoparticles (SLNs) (12, 13), and NLCs (14). All these formulations mainly focused on enhancing the oral bioavailability by improving the absorption or by lymphatic targeting to bypass the first-pass metabolism in order to reduce the dose strength. However, ritonavir is known to cause toxicity even at lower doses; hence, rescuing the pill burden may not address the main issue of ritonavir. Though the exact mechanism involved in the cause of hepatotoxicity induced by ritonavir is not clear, a raise in the reactive oxygen species (ROS) could be one of the reasons for it. Moreover, an increased level of ROS is associated with many other side effects. Hence, a novel formulation for ritonavir focused not only on the enhancement of its bioavailability but also on the capability to reduce toxicity is of utmost importance.

The normal functioning of cells results in the production of reactive nitrogen species (RNS) and ROS. Anti-oxidant enzymes such as superoxide dismutase (SOD), catalases, lactoperoxidase, glutathione peroxidoxin, and some anti-oxidant molecules such as vitamins (C and E), uric acid, glutathione, and bilirubin maintain a cellular balance and failure of which results in oxidative stress (15). Previously, Palipoch *et al.* reported protective effect of alpha-tocopherol combined with curcumin in cisplatin-induced hepatotoxicity in rats (16). In another study by Caddeo *et al.*, the anti-oxidant effect of alpha-tocopherol (vitamin E) was studied in *in vitro* studies (17). This emphasizes the importance of vitamin E intake for patients suffering from HIV infection.

Alpha-tocopherol is a natural anti-oxidant that belongs to the family of tocopherols and is commonly called vitamin E (18). It plays a crucial role in the maintenance of immune system (19). HIV infection not only affects the immune system but also lowers vitamin E levels which has been reported in patients infected with HIV infection. A diet history of HIV-positive patient consists of high intake of vitamin E (20). A non-concurrent prospective study conducted in the past reported that there might be a possible relation between high serum levels of vitamin E and slower HIV-1 disease progression (21). But vitamin E level decreases with disease progression in HIV-positive patients (19). And hence, there is a need for vitamin E supplement for the patients undergoing HIV treatment. In the current study, anti-oxidant-loaded NLCs of ritonavir were prepared using hot emulsion and ultrasonication method. Alpha-tocopherol was used as a source of anti-oxidant and also as liquid lipid in the preparation of NLCs to entrap ritonavir. As alpha-tocopherol is a well-known anti-oxidant, we hypothesized that it would help in improving the levels of anti-oxidant in the body and reduce the adverse effects of the drug by lowering the ROS levels.

MATERIALS AND METHODS

Chemicals and Reagents

Ritonavir was obtained as a gift sample from Dr. Reddy's Laboratories, Hyderabad, India. Lopinavir was a gift sample from Cipla Ltd., Mumbai, India. Stearic acid was procured from Finar Ltd., Ahmedabad, India. Glyceryl monostearate was purchased from Fine Organics, Mumbai, India. Alpha-tocopherol and oleic acid were purchased from Sigma-Aldrich, Bangalore, India. Sodium lauryl sulfate was purchased from Loba Chemie Pvt. Ltd. Tween 20 was procured from Merck, Mumbai, India. Strata™ X (10 mg/mL) cartridges were purchased from Phenomenex, Bangalore, India. Acetonitrile and methanol (HPLC grade) were purchased from SD Fine Chemicals, Mumbai. Ortho-phosphoric acid was purchased from Spectrochem Private Limited, Mumbai. Type-I water (ultrapure water) was obtained from water purifier system (Elix-Millipore Advantage, Millipore Corporation, Billerica, MA, USA).

Methods

Selection of Excipients for the Development of NLCs

For the selection of most suitable excipients for drug-loaded NLCs, the solubilizing ability towards ritonavir in different synthetic solid lipids (stearic acid, glyceryl monostearate (GMS), glyceryl di stearate, glyceryl tri-stearate, glyceryl palmito stearate, and palmitic acid) was tested. The maximum amount of drug dissolved in each lipid was determined by adding the drug in stepwise increasing order, under stirring, in the lipid thermostated above the melting point of the particular lipid. The solubility of the drug in each lipid was evaluated by visual observation for the presence of drug crystals and the formation of a transparent homogeneous system considered as the drug solubilized completely in that particular lipid (22). The solubility of the drug in different liquid lipids (oleic acid, castor oil, olive oil) was determined by adding a stepwise increment of a fixed amount of drug to different liquid lipids. The entire system was maintained under stirring, at a temperature of 80°C to mimic the actual experimental conditions of NLC preparation. After an equilibration period of 24 h, drug solubility in each system was evaluated visually. A homogenous and transparent system with the absence of drug crystals was considered as complete solubility of the drug (23). Solid lipids (stearic acid and GMS) and liquid lipids (oleic acid and alpha-tocopherol) were mixed in 90:10 w/w ratio. The mixture was heated for 30 min at 80°C and then allowed to cool at room temperature. The miscibility of selected solid lipid and liquid lipid was investigated by visual observation, and the absence of phase separation or turbidity was considered as the selected lipids were miscible (24). Different surfactants (Tween 20, Tween 40, Tween 60, Tween 80, SLS, poloxamer 188) were screened during the preparation of formulation. Mean PS (nm), PDI, and ZP (mV) were used as parameters to evaluate suitable surfactants.

Compatibility Studies

FTIR Analysis

Alpha II compact attenuated total reflectance-Fourier transform infrared (ATR-FTIR) spectrometer (Bruker) was used for the FTIR analysis of samples. In brief, zinc selenide crystal was cleaned using isopropanol and a small micro-spatula portion (15–20 mg) of solid sample was placed over it, so that it covers the ATR crystal. The anvil was gently pressed down till it makes contact with the sample. The anvil arm was rotated to ensure full contact between the sample and crystal. The spectra of the individual sample of pure drug, physical mixture of drug and excipients, and optimized formulation (batch I) were obtained after scanning at a wavelength range of 400–4000/cm (25).

DSC Analysis

Thermographic analysis of ritonavir pure drug and physical mixture of drug with excipients and optimized formulation (batch I) was performed using DSC analyzer (DSC 60 Plus, Shimadzu Corporation, Japan). In brief, 5 mg of sample was placed in a DSC pan, crimped, and heated at a rate of 10°C/min between 30 and 250°C in an inert gas atmosphere, with an empty DSC pan serving as a reference standard. The thermograms were recorded using companion software (26).

Preparation of NLCs with QbD Approach

Accurately weighed 50 mg of ritonavir was dissolved in a mixture of solid lipids (150/200 mg of stearic acid and 50 mg of GMS) and liquid lipid (15/25 μL of oleic acid and 15/25 μL of alpha-tocopherol), previously maintained at 80°C on a water bath. The aqueous phase/surfactant solution (Tween 20 (0.5/1% v/v) and SLS (0.25% w/v)) maintained at 80°C was added to the melted lipid-drug matrix to form an emulsion (o/w), and it was sonicated at 30 ± 2% amplitude for 5 min with the help of probe sonicator (Ultrasonic Processor VC130, Sonics and Materials Inc., USA). The sonicated emulsion was chilled down on an ice bath and was stored at 4°C for further analysis (27).

QTPP

The QbD approach was followed to produce a high-quality product with the enhancement of its efficacy. The quality target product profile (QTPP) was defined as shown in Table I (28).

Risk Assessment of CQAs

For identification of potential risks and possible variables for failure of the product, risk assessment of CQAs was performed by constructing Ishikawa diagram (Figure 1). This approach fulfills the requirements of ICH Q9 guidelines and helps in enhancement of the quality, efficacy, and safety of the product. Ishikawa diagram represents the possible variables that can affect the responses or critical quality attributes (CQAs) (such as PS, PDI, ZP, and EE) and are defined based on prior knowledge, preliminary trials, and literature. Furthermore, for risk assessment, failure mode effects analysis (FMEA) was followed. All the possible variables (critical method parameters (CMPs) and critical process parameters (CPPs)) that could affect CQAs were listed, and risk ranking was given as low, medium, and high (Table II) (28, 29).

Screening Design

All the possible variables are listed in Table II, and the variables with high impact on the responses were further selected based on the risk categories. Furthermore, to confirm the statistical effect of these variables on responses, a screening design (Plackett-Burman model) was created using a software (Design Expert® v.9.0.5.1.) and the selected variables were studied at two different levels. Variables with their different levels are given in Table III, and experiments suggested by software with the Placket-Burman design are given in Table IV. All trials suggested by the software were prepared and responses (PS, PDI, and ZP) were recorded. Statistical calculations were performed using the software to understand the effect of each variable on measured responses.

Optimization of Formulation

The most influential factors from the independent variables selected for the screening design were identified based on the results of screening trials. These variables were further optimized using central composite design (CCD) created using Design Expert® software. The selected variables with levels are presented in Table V. And the details of different compositions of trials suggested by the software are

Table I Study Target with Justification

QTPP	Targets	Justification
Route of administration	Oral route	• Convenient route of delivery
Type of formulation	Nanoparticles	• Small size particles can help in site-specific delivery. • Lipid nanoparticles can help to reduce hepatic exposure due to ritonavir. • Lipid nanoparticles can help to enhance the drug uptake by the lymphatic system.
Targeting	Site-specific delivery to the lymphatic system	• Lymphatic targeting is selected to avoid first-pass metabolism.
Reduce toxicity	Reduce hepatotoxicity	• Lymphatic targeting and incorporation of anti-oxidant can help in reducing the hepatotoxicity of ritonavir.

QTPP quality target product profile

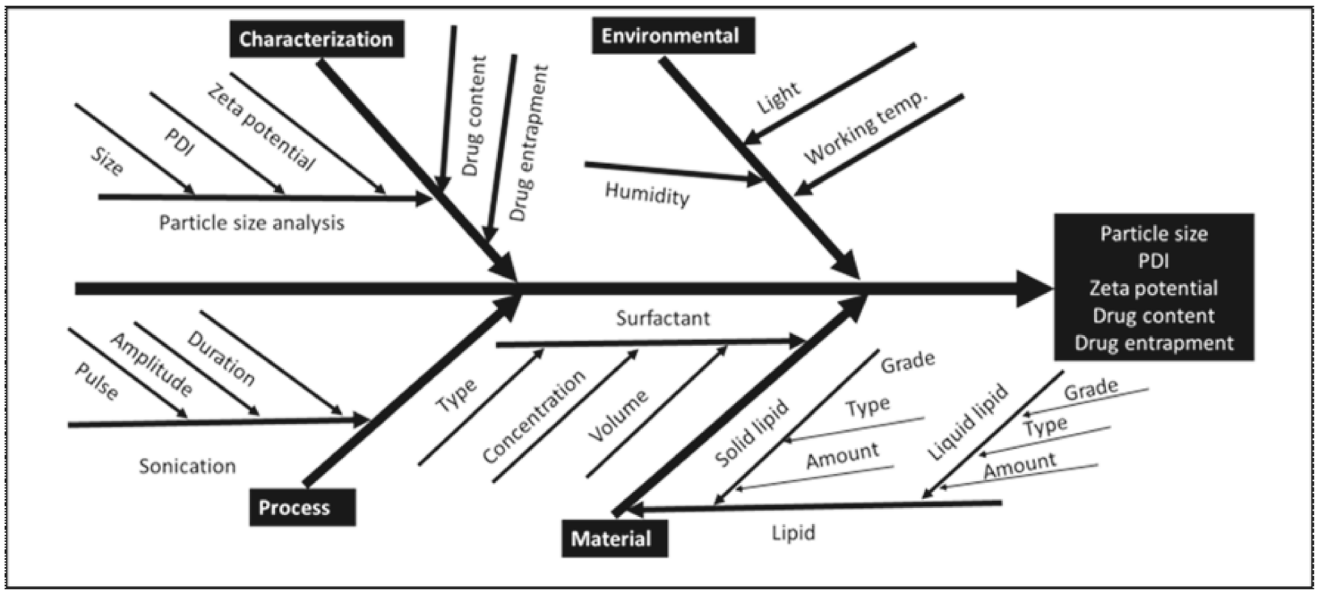

Fig. 1 Ishikawa diagram demonstrating various possible independent variables on critical quality attributes

listed in Table VI. PS, PDI, ZP, and EE were measured as the responses for all the trials.

Validation of Software-Suggested Formulations

After preparing all the batches suggested by the software in the optimization design, data was entered into the software, and based on the selected criteria, the software suggested a few solutions consisting of formulation composition, predicted responses (PS, PDI, ZP, and EE), and desirability values. Out of all, three formulation compositions (batch I, batch II, and batch III) with the most suitable composition and desirability value were selected, and formulation batches were prepared and analyzed for responses. The residual errors were calculated from the experimental and predicted responses.

Process Analytical Technology (PAT)

PS, PDI, and ZP of the formulations were determined using Zeta-sizer (Malvern Zeta Sizer Nano- ZS90, Malvern Instruments Ltd., UK) at an optical arrangement of detector at 173° and ambient temperature of 25°C after diluting the formulation samples adequately using Milli-Q water. HPLC (LC-2010CHT model, Shimadzu Corporation, Kyoto, Japan) was used for the determination of drug EE. In brief, Inertsil

Table II Risk Assessment Using FMEA

S. no.	Risk factor	Particle size	PDI	Zeta potential
1	Type of solid lipid	High	High	High
2	Grade of solid lipid	Medium	Medium	Low
3	Amount of solid lipid	High	High	High
4	Type of liquid lipid	Medium	Medium	Low
5	Grade of liquid lipid	Low	Low	Low
6	Amount of liquid lipid	High	Medium	Low
7	Type of surfactant	High	High	High
8	Concentration of surfactant	High	High	High
9	Volume of surfactant	High	High	Low
10	Sonication time	High	High	Medium
11	Sonication amplitude	Medium	Medium	Low
12	Sonication pulse	Medium	Medium	Low
13	Sonication probe temperature	Medium	Medium	Low
14	Light	Low	Low	Low
15	Ambient temperature	Low	Low	Low
16	Humidity	Low	Low	Low
17	Analyst	Low	Low	Low
18	Source of water	Low	Low	Low
19	Software	Low	Low	Low

PDI polydispersity index

Table III Independent Variables with Levels Selected for the Screening Trials

S. no.	Independent variables	Levels	
		−1	+1
1	Amount of solid lipid (GMS) (mg)	100	200
2	Amount of solid lipid (stearic acid) (mg)	100	200
3	Amount of liquid lipid (oleic acid) (μL)	10	20
4	Amount of liquid lipid (alpha-tocopherol) (μL)	10	20
5	Surfactant concentration (Tween 20) % v/v	0.875	1.750
6	Surfactant concentration (SLS) % v/v	0.125	0.25
7	Volume of aqueous phase (mL)	10	20
8	Sonication time (min)	05	07
9	Sonication pulse (sec)	04	08
10	Sonication amplitude strength (%)	30	40
11	Sonication probe temperature (°C)	25	40

GMS glyceryl monostearate, *SLS* sodium lauryl sulfate

ODS-3V C18 column (250 × 4.6 mm, 5 μm particle size with a pore size of 100 Å) was used as a stationary phase and mobile phase consisting of acidified type-I water (pH adjusted to 3 with ortho-phosphoric acid) and acetonitrile in the ratio 40:60, % v/v, was pumped at a flow rate of 1.2 mL/min for 12 min for each sample. The chromatograms were recorded and analyzed using the software, Lab Solutions v.5.57. For total drug content, methanol was added to the formulation to dissolve the lipid content and sonicated for 10 min using a bath sonicator (Ultrasonic Cleaner, Equitron-Medica Instrument Mfg. Co., Mumbai, India). Furthermore, appropriate dilutions were made using methanol and analyzed using a validated HPLC analytical method. For separation of free and entrapped drug from the formulations, solid-phase extraction method was followed using Strata- X, 1 mL (Phenomenex) cartridge, the procedure of which is schematically represented in Figure 2 (30, 31). To the samples collected for the analysis of entrapped drug, methanol was added to dissolve the lipid and sonicated for 10 min followed by appropriate dilution with methanol and quantified using HPLC. The samples collected for the free drug analysis were diluted appropriately using methanol and analyzed using HPLC. The drug EE was calculated from the following formula.

$$\%EE = (\text{Amount of entrapped drug}/\text{Amount of total drug content}) \times 100$$

Table V Variables with Levels Selected for NLC Optimization Design

S. no.	Variable	Level	
		−1	+1
1	Amount of solid lipid (GMS) (mg)	150	200
2	Amount of liquid lipid (oleic acid) (μL)	15	25
3	Amount of liquid lipid (alpha-tocopherol) (μL)	15	25
4	Surfactant concentration (Tween 20) (% v/v)	0.5	1

GMS glyceryl monostearate

In Vitro Drug Release Studies

Drug release studies of NLCs (batch I, batch II, and batch III) and pure drug in two different buffers, 0.1 N HCl and phosphate buffer pH 6.8, were conducted using dissolution apparatus (USP type-II). Accurately, 2 mL of the prepared formulation was loaded into a dialysis bag with MWCO 12000 kDa (Dialysis Membrane-150 (LA 401-5MT), HIMEDIA) and placed in 500 mL of respective buffer in a dissolution jar. For standard, 10 mg of ritonavir API was

Table IV Placket-Burman Design for the Screening of Independent Variables

S. no.	Amount of solid lipid		Amount of liquid lipid		Surfactant			Sonicator parameters				Responses (mean ±*SD*,*n*= 3)		
	A	B	C	D	E	F	G	H	I	J	K	Particle size (nm)	PDI	Zeta potential (mV)
1	200	100	20	20	0.875	0.25	20	7	4	30	25	236.00 ± 6.42	0.442 ± 0.05	−34.37 ± 1.84
2	100	200	10	20	1.750	0.125	20	7	8	30	25	1764.00 ± 180.55	0.891 ± 0.09	−43.17 ± 0.8
3	200	200	20	10	0.875	0.125	20	5	8	40	25	973.37 ± 105.08	0.594 ± 0.14	−43.87 ± 0.96
4	100	100	10	20	0.875	0.25	20	5	8	40	40	1086.57 ± 334.8	0.839 ± 0.1	−41.57 ± 4.89
5	200	100	20	20	1.750	0.125	10	5	8	30	40	265.37 ± 76.09	0.507 ± 0.05	−42.53 ± 0.91
6	200	100	10	10	1.750	0.125	20	7	4	40	40	1854.67 ± 412.41	0.96 ± 0.07	−31.3 ± 1.04
7	100	200	20	20	0.875	0.125	10	7	4	40	40	858.00 ± 32.71	0.63 ± 0.12	−45.9 ± 0.89
8	200	200	10	10	0.875	0.25	10	7	8	30	40	1093.67 ± 115.58	0.706 ± 0.06	−41.83 ± 2.84
9	200	200	10	20	1.750	0.25	10	5	4	40	25	1494.67 ± 70.21	0.781 ± 0.07	−43.4 ± 0.95
10	100	100	10	10	0.875	0.125	10	5	4	30	25	890.83 ± 21.81	0.676 ± 0.07	−42.43 ± 2.15
11	100	100	20	10	1.750	0.25	10	7	8	40	25	1954.67 ± 610.95	0.946 ± 0.05	−41.77 ± 2.51
12	100	200	20	10	1.750	0.25	20	5	4	30	40	1557.00 ± 261.08	0.871 ± 0.14	−44.17 ± 1.63

A, GMS (mg); B, stearic acid (mg); C, oleic acid (μL); D, alpha tocopherol (μL); E, Tween 20 (% v/v); F, SLS (% w/v); G, volume of aqueous phase (mL); H, sonication time (min); I, sonication pulse (sec); J, amplitude (%); K, probe temperature (°C)
SD standard deviation, *PDI* polydispersity index

Table VI Central Composite Design (Small) for the Optimization of Formulation Design

S. no.	Run no.	Factors				Responses			
		A	C	D	E	Particle size (nm) (mean ±*SD*,*n*= 3)	PDI (mean ±*SD*,*n*= 3)	Zeta potential (mV) (mean ±*SD*,*n*= 3)	Entrapment efficiency (%)
1	Run 01	132.96	20.00	20.00	0.75	338.63 ± 48.13	0.43 ± 0.10	−41.77 ± 3.5	74.51
2	Run 02	200.00	25.00	25.00	0.50	310.40 ± 60.08	0.41 ± 0.11	−41.63 ± 4.84	66.88
3	Run 03	175.00	20.00	28.41	0.75	458.67 ± 14.32	0.45 ± 0.02	−48.27 ± 4.06	66.87
4	Run 04	150.00	15.00	25.00	0.50	360.93 ± 109.01	0.41 ± 0.10	−48.40 ± 7.01	62.70
5	Run 05	175.00	20.00	20.00	0.75	280.93 ± 56.38	0.35 ± 0.08	−46.20 ± 4.33	74.12
6	Run 06	200.00	15.00	25.00	1.00	334.40 ± 50.11	0.43 ± 0.11	−42.50 ± 3.24	64.77
7	Run 07	175.00	20.00	20.00	1.17	258.53 ± 8.44	0.44 ± 0.03	−46.5 ± 2.96	65.20
8	Run 08	150.00	25.00	25.00	1.00	353.47 ± 36.17	0.48 ± 0.01	−42.47 ± 4.14	58.84
9	Run 09	150.00	25.00	15.00	1.00	288.20 ± 15.23	0.42 ± 0.04	−42.13 ± 3.11	53.99
10	Run 10	175.00	20.00	20.00	0.33	344.13 ± 38.16	0.46 ± 0.02	−52.23 ± 5.26	53.18
11	Run 11	175.00	28.41	20.00	0.75	338.83 ± 27.25	0.39 ± 0.09	−48.77 ± 1.63	68.42
12	Run 12	217.05	20.00	20.00	0.75	288.03 ± 25.23	0.41 ± 0.09	−44.77 ± 0.4	67.08
13	Run 13	175.00	11.59	20.00	0.75	273.87 ± 2.28	0.39 ± 0.06	−45.27 ± 1.03	64.62
14	Run 14	175.00	20.00	20.00	0.75	294.43 ± 23.01	0.42 ± 0.03	−46.73 ± 2.72	60.30
15	Run 15	200.00	25.00	15.00	0.50	304.10 ± 22.40	0.43 ± 0.06	−45.47 ± 3.05	62.00
16	Run 16	200.00	15.00	15.00	1.00	324.00 ± 58.47	0.46 ± 0.07	−40.93 ± 4.93	57.71
17	Run 17	175.00	20.00	20.00	0.75	356.63 ± 36.84	0.41 ± 0.06	−45.43 ± 6.37	66.51
18	Run 18	150.00	15.00	15.00	0.50	352.10 ± 27.56	0.43 ± 0.10	−44.97 ± 3.06	57.40
19	Run 19	175.00	20.00	11.59	0.75	324.70 ± 62.10	0.33 ± 0.08	−45.47 ± 2.84	72.78
20	Run 20	175.00	20.00	20.00	0.75	234.17 ± 13.19	0.31 ± 0.01	−46.47 ± 6.56	52.57
21	Run 21	175.00	20.00	20.00	0.75	375.37 ± 31.50	0.32 ± 0.01	−47.2 ± 4.94	47.37

A, solid lipid (GMS*) (mg); C, liquid lipid (Oleic acid) (μL); D, liquid lipid (alpha-tocopherol) (μL); E, surfactant concentration (Tween 20) (% v/v)
SD standard deviation, *PDI* polydispersity index

added to 2 mL of surfactant solution (0.9% v/v of Tween 20 in 0.250% w/v of SLS) to make a suspension and loaded into a dialysis bag. A controlled temperature (37 ± 0.5°C) and rotation of paddle (50 ± 1 rpm) were maintained throughout the study. Samples (1 mL) were withdrawn from the basket at specified time intervals, and the volume was replenished with the same amount of buffer. The concentration in all the collected samples was determined using HPLC after filtration and appropriate dilution of the samples.

FESEM Analysis

Surface morphology studies were performed for the optimized NLCs (batch I). Prior to FESEM analysis, NLCs were lyophilized using Christ alpha-2 freeze dryer using mannitol (5% w/v) as cryoprotectant. Briefly, lyophilized NLCs powder was placed on a copper stud and sputter-coated with gold and analyzed in FESEM instrument under accelerating voltage (30 kV). Images were captured at different magnifications.

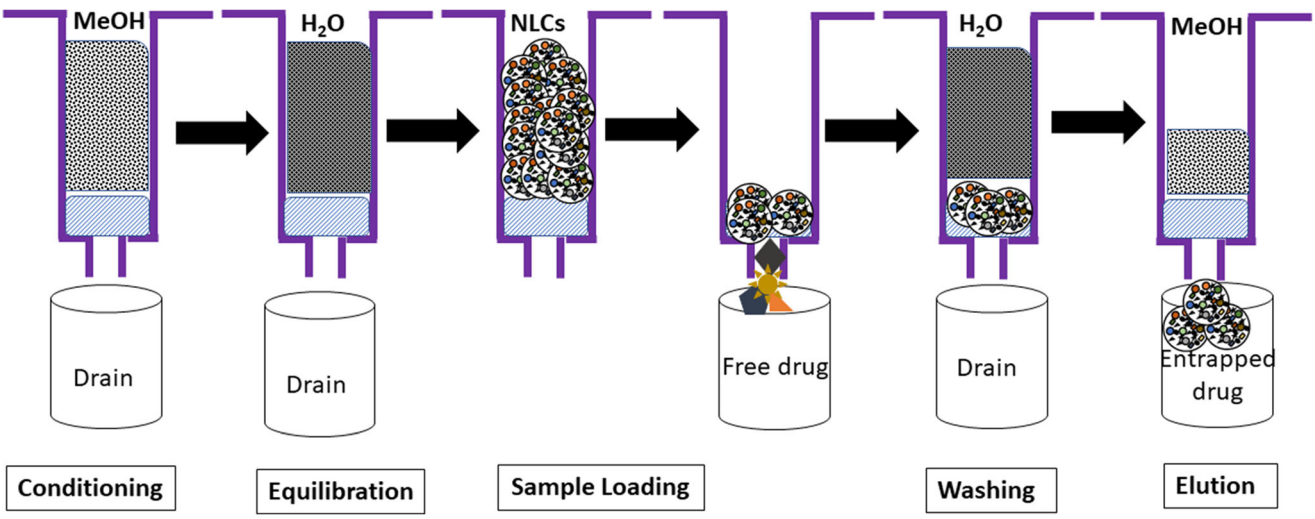

Fig. 2 Schematic representation of protocol for solid-phase extraction

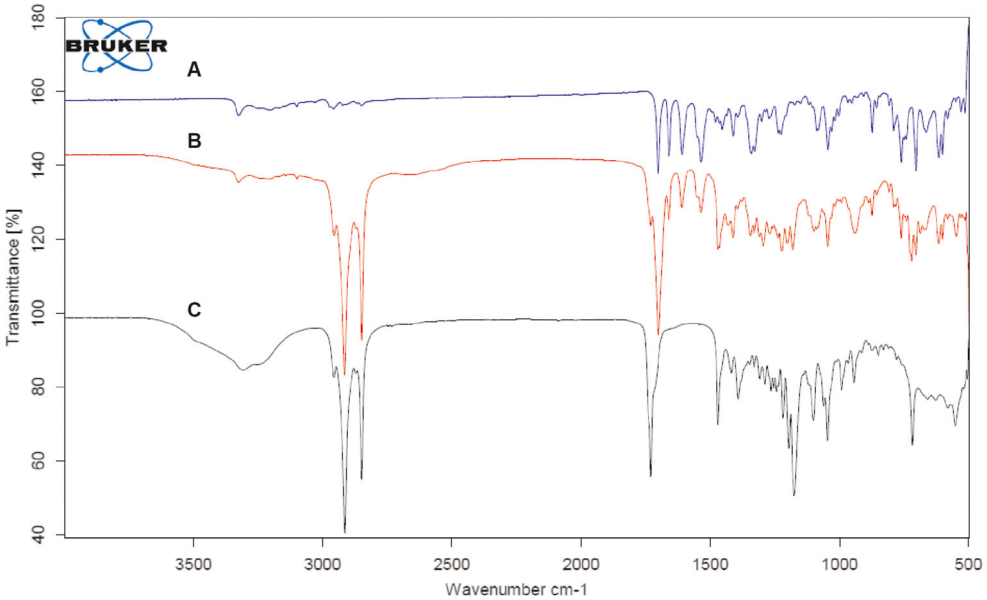

Fig. 3 FTIR spectrum of the pure drug (**A**), physical mixture(**B**), and optimized formulation (**C**)

Pharmacokinetics of the Optimized Formulation

Animals. Pharmacokinetic evaluation of NLCs was conducted in male Wistar rats weighing between 200 and 250 g. Animals were inbred at Central Animal Research Facility, Manipal Academy of Higher Education (MAHE), Manipal. Animals were housed in polypropylene cages provided with sterile husk and under controlled temperature (23 ± 3 °C) and humidity conditions. All the animal studies (Institutional animal ethical clearance No. IAEC/KMC/51/2018) were carried out at Central Animal Research Facilities (CARF), MAHE, Manipal, as per the CPCSEA norms (registration no. 94/1999 CPCSEA and MCOPS registration no. 6/2011 CPCSEA, Manipal).

Study Design. Animals were divided into three groups (group I, group II, and group III) with six animals in each group. All the animals were fasted overnight before experimenting. Group I was dosed orally with ritonavir pure drug suspension (50 mg/kg/10 mL). Group II animals were dosed with a suspension of marketed formulation of ritonavir (Ritomune, 50 mg/kg/10 mL) orally. And group III animals

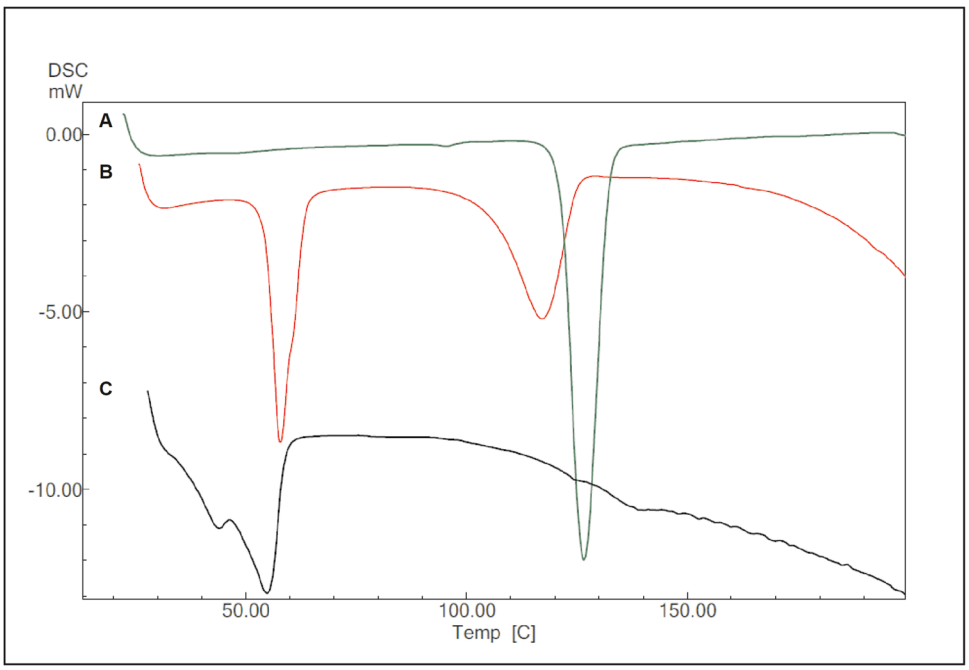

Fig. 4 DSC thermogram of ritonavir (**A**), physical mixture of ritonavir and excipients (**B**), and optimized formulation (**C**)

Table VII The Statistical Values of Independent Variables Effect on the Responses

S. no.	Factor	Level		Particle size (nm)		PDI		Zeta potential (mV)	
		−1	+1	*p*value	Coefficient	*p*value	Coefficient	*p*value	Coefficient
1	A	100	200	0.04	−182.84	0.015	−0.08	0.003	1.78
2	B	100	200	0.09	121.13	0.072	0.02	0.002	−2.33
3	C	10	20	0.04	−195.08	0.019	−0.06	0.016	−0.78
4	D	10	20	0.03	−218.37	0.026	−0.05	0.039	−0.50
5	E	0.875	1.75	0.02	312.74	0.015	0.08	0.119	0.27
6	F	0.125	0.25	0.22	67.96	0.016	0.02	0.187	0.20
7	G	10	20	0.18	76.12	0.058	0.02	0.004	1.63
8	H	5	7	0.08	124.36	0.036	0.03	0.004	1.67
9	I	05/02	08/02	-	-	-	-	0.338	−1.13
10	J	30	40	0.0340	201.34	0.0193	0.063	-	-
11	K	25	40	-	-	0.0516	0.024	-	-

A, GMS (mg); B, stearic acid (mg); C, oleic acid (μL); D, alpha tocopherol (μL); E, Tween 20 (% v/v); F, SLS (% w/v); G, volume of aqueous phase (mL); H, sonication time (min); I, sonication pulse (sec); J, amplitude (%); K, probe temperature (°C)
PDI polydispersity index

were dosed with optimized NLCs (batch I) of ritonavir (50 mg/kg/10 mL) by oral route. Approximately 0.25 mL of blood was withdrawn from each animal at different time points and collected into tubes with an anti-coagulant. All the samples were centrifuged, and plasma was separated. Drug concentration in all the samples were estimated using HPLC bioanalytical method.

Extraction of Ritonavir from Rat Plasma Samples. A simple bioanalytical method was developed for the extraction and quantification of ritonavir in plasma samples. Protein precipitation method was used for the extraction of ritonavir from plasma samples. Briefly, to 50 μL of plasma, 20 μL of internal standard (lopinavir, 200 μg/mL) and 150 μL of chilled methanol were added to precipitate the samples. Furthermore, all samples were vortexed, centrifuged at 15,000 rpm, 4°C for 10 min. Finally, the supernatant was separated and analyzed using HPLC. The chromatographic conditions for bioanalysis of the sample includes mobile phase combination of methanol and acidified Milli-Q water (pH adjusted to 3.0 using 20% orthophosphoric acid) in a ratio of 85:15, % v/v. Kromasil C18 (250 × 4.6 mm, 5 μm) column was used for

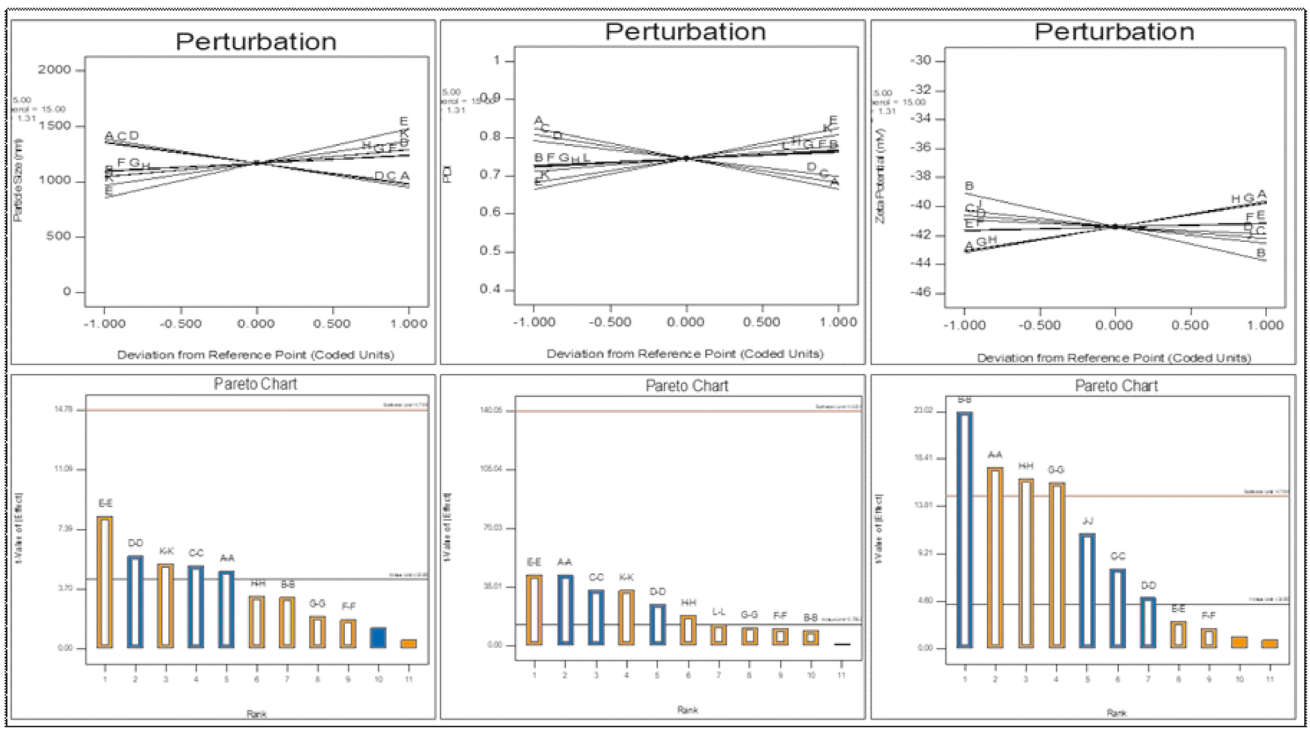

Fig. 5 Perturbation and pareto charts for effect of different variable on the responses in screening trials performed using Plackett-Burman design. A, GMS (mg); B, stearic acid (mg); C, oleic acid (μL); D, alpha tocopherol (μL); E, Tween 20 (% v/v); F, SLS (% w/v); G, volume of aqueous phase (mL); H, sonication time (min); J, sonication pulse (sec); K, amplitude (%); L, probe temperature (°C)

Table VIII ANOVA for Response Surface Reduced Quadratic Model for Various Responses

Factor	Coefficient of estimate	P value	Polynomial equation
Particle size			
C	2.95	0.686	Particle Size = +321.64 + 2.95*C - 11.36*D + 20.05*C^2 + 18.09*D^2
D	-11.36	0.133	
C^2	20.05	0.010	
D^2	18.09	0.018	
R^2	0.52		
Adjusted R^2	0.40		
Pred R-Squared	-0.22		
Adeq Precision	5.44		
PDI			
A	-0.014	0.256	PDI = + 0.46 - 0.014*A - 0.006*B + 0.03*C - 0.04*A^2 - 0.02*B^2
B	-0.006	0.623	
C	0.034	0.013	
A^2	-0.036	0.007	
B^2	-0.022	0.077	
R^2	0.600		
Adjusted R^2	0.467		
Pred R-Squared	-0.136		
Adeq Precision	7.711		
Zeta potential			
A	-0.11	0.93	Zeta Potential = -60.69 - 0.11*A + 3.27*A^2
A^2	3.27	0.01	
R^2	0.32		
Adjusted R^2	0.24		
Pred R-Squared	-0.31		
Adeq Precision	5.68		
Entrapment efficiency			
A	-4.05	0.10	Entrapment = + 37.83 - 4.05*A + 8.57*B + 0.94*C + 5.50*D + 8.60*AB - 4.64*AC + 6.34*AD + 5.48*BC - 7.25*BD + 2.03*CD - 1.55*A^2 + 5.41*B^2 + 1.32*C^2 - 1.23*D^2
B	8.57	0.01	
C	0.94	0.51	
D	5.50	0.04	
AB	8.60	0.02	
AC	-4.64	0.04	
AD	6.34	0.06	
BC	5.48	0.02	
BD	-7.25	0.04	
CD	2.03	0.29	
A^2	-1.55	0.27	
B^2	5.41	0.01	
C^2	1.32	0.34	
D^2	-1.23	0.38	
R^2	0.93		
Adjusted R^2	0.76		
Pred R-Squared	-0.88		
Adeq Precision	10.25		

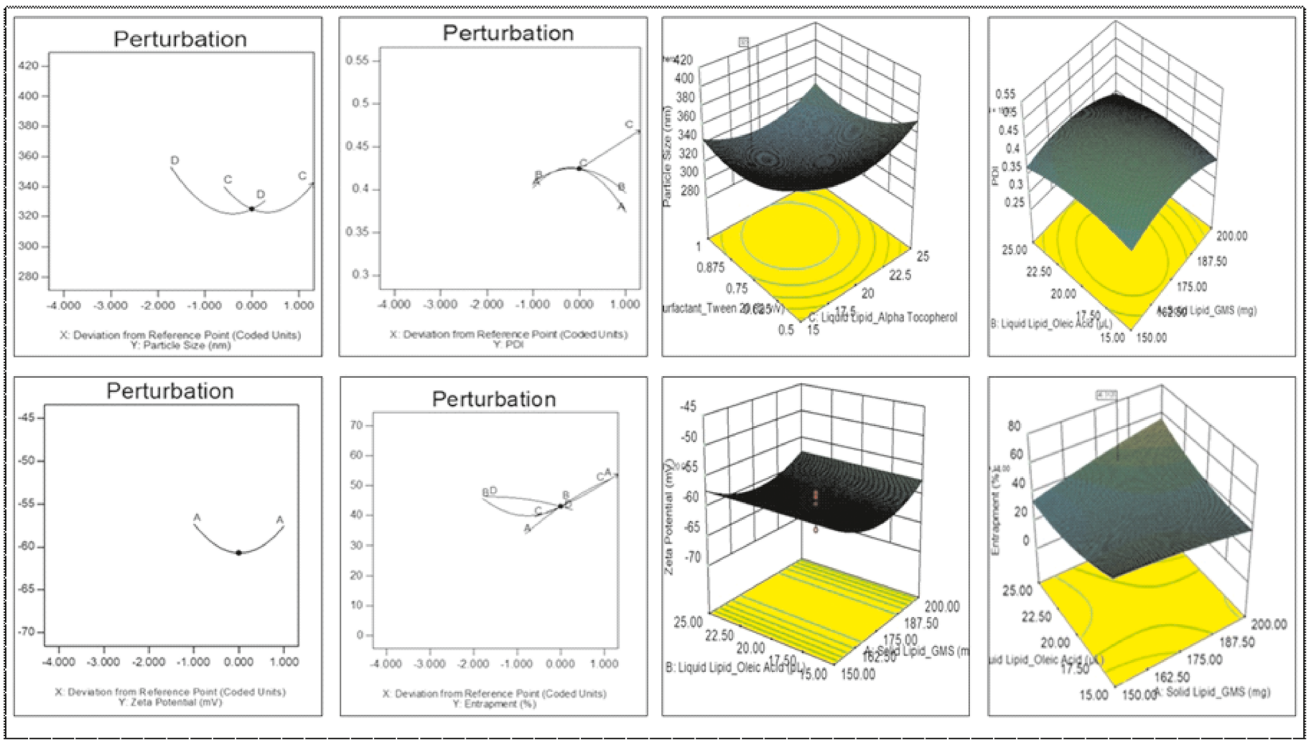

Fig. 6 Optimization of formulation using CCD model, perturbation and response surface plots for the effect of different variable on responses. A, GMS (mg); B, stearic acid (mg); C, oleic acid (µL); D, alpha tocopherol (µL); E, Tween 20 (% v/v); F, SLS (% w/v); G, volume of aqueous phase (mL); H, sonication time (min); J, sonication pulse (sec); K, amplitude (%); L, probe temperature (°C)

chromatographic separation. The temperature of the column was maintained at 25°C, and the flow rate was set to 1.200 mL/min. Total run time was set to 12 min, and column effluents were monitored at 242 nm to record the response.

RESULTS

Formulation Development

Based on drug intake and solubility in different solid lipids, stearic acid and GMS showed the highest solubilizing ability among all the investigated solid lipids. Stearic acid (100 mg) and GMS (100 mg) were able to solubilize up to 37.5 and 27.5 mg of ritonavir. Therefore, a combination of GMS and stearic acid was used for the development of NLCs in the present study. Furthermore, Tween 20 and SLS were selected as surfactants for the formulation development. Oleic acid was selected as liquid lipid as it showed better intake than the other liquid lipids screened, and along with that, alpha-tocopherol was used as liquid lipid and also as an anti-oxidant in the preparation of NLCs.

Drug-Excipient Compatibility Studies

Drug and excipient compatibility was confirmed with DSC and FTIR studies. The IR spectrum of ritonavir showed characteristic absorption peaks at 1085.20/cm for C–O, 1225.27/cm for CH_2 rock, 1454.04/cm CH_3 for a scissor,

Table IX Verification of Optimized Parameters Suggested by the Software

S. no.	Batch no.	Variables				Desirability	Response (mean ±*SD*,*n*= 3)							
		A	*B*	*C*	*D*		Particle size (nm)		PDI		Zeta potential (mV)		Entrapment efficiency (%)	
							*	#	*	#	*	#	*	#
1	I	174.12	24	18	0.93	0.94	325.00	362.1 ± 27.57	0.426	0.431 ± 0.05	−60.70	−56.40 ± 10.43	44.43	46.40 ± 4.00
2	II	170.02	24	18	0.91	0.92	323.83	356.50 ± 18.79	0.427	0.443 ± 0.03	−60.54	−48.70 ± 0.60	43.20	45.37 ± 4.45
3	III	180.00	24	18	0.90	0.91	323.39	357.40 ± 12.97	0.420	0.420 ± 0.05	−60.59	−52.10 ± 2.15	46.75	45.43 ± 8.94

A, GMS (mg); B, oleic acid (µL); C, alpha tocopherol (µL); D, Tween 20 concentration (% v/v); *, software predicted values; #, experimental values
SD standard deviation, *PDI* polydispersity index

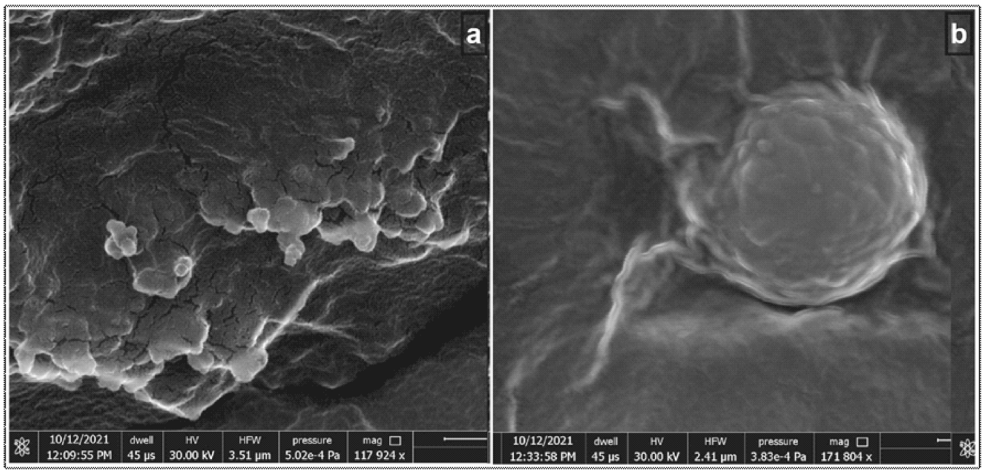

Fig. 7 FESEM results of optimized formulation at different magnifications (scale: 1 µm (**a**) and 500 nm (**b**))

1607.83/cm for –CH_3–, 1701.14/cm for CO_2, 2834.91/cm for CH_2 asymmetric stretching, 3030.17/cm for –C– aryl stretching, and 3322.94/cm for COOH stretch. The presence of characteristic peaks in pure drug and the physical mixture confirms the compatibility of drug and other excipients that are intended to use in the preparation of formulation (Figure 3 represents the FTIR spectroscopical images of the pure drug, physical mixture, and optimized formulation). The DSC thermogram of pure ritonavir (Figure 4A) showed a sharp endothermic peak at 126.59°C, physical mixture (Figure 4B) at 117.04°C, and lyophilized powder of optimized formulation not showing any drug peak due to complete entrapment of drug in lipids (Figure 4C).

Preparation of Nanostructured Lipid Carriers with QbD Approach

Hot emulsification and probe sonication method were employed in the current study for the development of NLCs. An added advantage of this technique is that it does not involve the usage of organic solvents, thereby circumventing the toxicity produced by the organic solvents in comparison to other methods such as emulsification-solvent evaporation solvent injection methods. Moreover, this method is simple and less laborious (32).

CMAs and CPPs were defined, and the Ishikawa diagram was useful in scrutinizing various possible factors that could affect the CQAs of the final product. Furthermore, FMEA approach was followed to prioritize the factors that should be taken for the screening trials. The effect of various factors was assessed for the determination of the most influential variable that affects CQAs using Plackett-Burman model. The responses collected for the trials suggested by the model are presented in Table IV, and ANOVA statistics is given in Table VII. Stearic acid was not having any major impact on PS and PDI, and very minimal effect on zeta potential, and hence, it was not selected for further optimization. Similarly, sonication parameters (H, I, J, K) were also found to have minimal or no effect on the responses. GMS, oleic acid, and alpha-tocopherol exhibited significant effects on all three responses and Tween 20 on PS and PDI. Based on the screening data, factors A, C, D, and E were further optimized using central composite model. Perturbation and pareto charts explaining the effect of variables on responses are presented in Figure 5.

Optimization of Formulation and Verification of Results

The central composite design was implemented for the screening of variables to determine the main and interactive effects of four variables (amount of GMS, oleic acid, alpha-

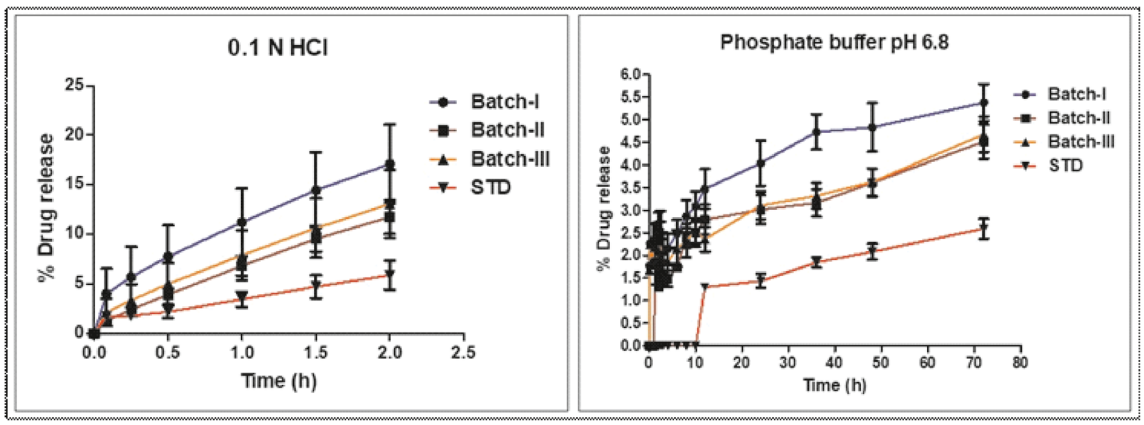

Fig. 8 In vitro drug release profile of formulation batches and standard drug in different buffers

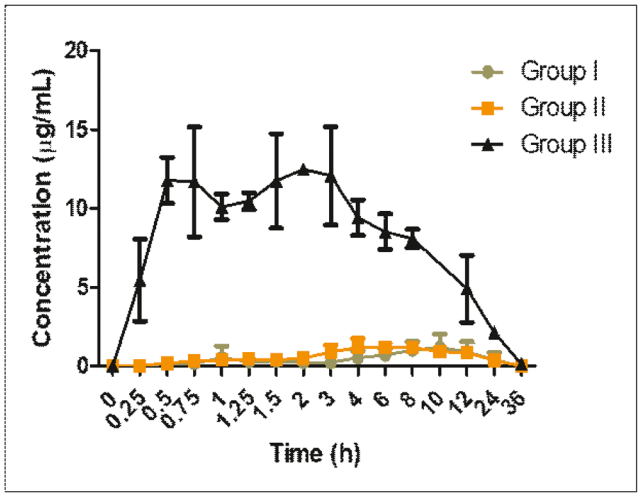

Fig. 9 Time *vs* plasma concentration of ritonavir pure drug suspension and optimized formulation in rats after oral administration. Group I, pure drug suspension, 50 mg/kg, oral; Group II, marketed formulation suspension, 50 mg/kg, oral; Group III, optimized formulation, 50 mg/kg, oral

tocopherol, and concentration of Tween 20) on four responses (CQAs, i.e., PS, PDI, ZP, and EE), and results are presented in Table VI. The responses were further input into the software, and ANOVA calculations were performed to understand the interactive effect of the variables on the quality of the product; the data is presented in Table VIII, and the interactive effect of variables on responses is presented in Figure 6. To verify the solutions suggested by the software, the formulation batches were prepared and the responses collected are presented in Table IX.

PAT Analysis

Ritonavir-loaded nanostructured lipid carriers were developed employing QbD during the screening and optimization of the formulation. For screening trials, PS was found to be in the range of 235.1 to 1954.7 nm, PDI of 0.442 to 0.960, and ZP in the range of − 45.9 to −31.3 mV. Similarly, for optimization trials, PS was in the range of 273.9 to 458.7 nm, PDI was in the range of 0.314 to 0.480, ZP was found in the range of −52.2 to − 40.9 mV, and encapsulation efficiency was in the range of 47.37 to 74.51%.

FESEM Analysis

The particle size obtained with FESEM analysis was close to the results obtained with zeta sizer. The images of FESEM analysis are given in Figure 7. The shape of the nanoparticles of ritonavir-loaded NLCs appeared spherical with smooth surface and the size was found to be between 250 and 370 nm.

In Vitro Drug Release Studies

In vitro drug release study was performed for standard drug and all the three validated formulation batches (batches I, II, and III) in 0.1 N HCl buffer for 2 h and phosphate buffer pH 6.8 for 72 h, and the data is presented in Figure 8. In phosphate buffer pH 6.8, it was observed that during the first 12 h, there was no drug release from the standard group, whereas release was observed 15 min onwards in batch I and II formulations and 2 h onwards from batch III formulation. From all batches of formulations and standard, the drug release was found to be higher in 0.1 N HCl compared to phosphate buffer pH 6.8.

Pharmacokinetic Studies

The concentration of ritonavir in plasma at different time points was determined using bioanalytical HPLC method, and a time-plasma concentration graph was constructed for different treatments (Figure 9). The pharmacokinetic parameters such as T_{max}, C_{max}, half-life, elimination rate constant, AUC, clearance, volume of distribution, and mean residence time were calculated using the Win-nonlin software, and the data is presented in Table X.

DISCUSSION

Hepatotoxicity is a major adverse effect seen in patients with ritonavir treatment and is concentration-dependent also. However, the exact mechanism behind hepatotoxicity induced by ritonavir is not known but its severity is mainly assessed by sensing the elevated concentrations of aspartate aminotransferase (AST) and alanine aminotransferase (ALT) enzymes of the liver (10). Coagulopathy, jaundice, or encephalopathy is considered as a general definition of severe

Table X PK Parameters of Various Treatments in Rats After Single-Dose Oral Administration

S. no.	Parameter	Group I (mean ±*SD*,*n*= 6)	Group II (mean ±*SD*,*n*= 6)	Group III (mean ±*SD*,*n*= 6)
1	AUC (hr µg/mL)	18.72 ± 8.75	20.69 ± 3.48	159.5437 ± 36.20
2	C_{max} (µg/mL)	1.19 ± 0.67	1.19 ± 0.09	12.4672 ± 1.0
2	T_{max} (h)	10.00 ± 1.79	8.00 ± 3.77	2.00 ± 0.37
4	Half-life (h)	9.51 ± 5.41	10.70 ± 5.13	5.67 ± 3.58
5	K_e (1/h)	0.07 ± 0.03	0.06 ± 0.04	0.12 ± 0.07
6	V_d (mL/kg)	31371.12 ± 10029.81	31,796.26 ± 12,223.66	2547.84 ± 474.77
7	Cl (mL/h/kg)	2287.43 ± 1485.20	2059.69 ± 723.82	311.24 ± 46.07
8	MRT (h)	18.22 ± 8.79	17.32 ± 6.81	9.9137 ± 4.54

Group I, pure drug suspension, 50 mg/kg, oral; Group II: marketed formulation suspension, 50 mg/kg, oral; Group III: optimized formulation, 50 mg/kg, oral
SD standard deviation, *AUC* area under the curve, *MRT* mean residence time

liver injury (33). Hepatotoxicity caused by a full dose of ritonavir (400 mg twice a day along with saquinavir or 600 mg of ritonavir alone twice a day) was independent of coinfection with chronic hepatitis. And it is also identified as an independent risk factor for the development of severe hepatotoxicity (grade 3 or 4) among all other PIs (34). Apart from hepatotoxicity, treatment with PIs was also associated with a significant rise in total cholesterol levels and it is more pronounced in treatment with ritonavir in comparison with other PIs (35). It was demonstrated that ritonavir at concentrations near clinical plasma levels increases cytotoxicity in human endothelial cell cultures and decreases cell viability in a time and dose-dependent manner. Mitochondrial DNA damage was also evidenced by ritonavir treatment. And data suggest that ritonavir can cause endothelial cell injury, which may be linked to cardiovascular complications associated with its clinical applications (36, 37). It was demonstrated that ritonavir at a dose of 100 mg twice daily, which is not sufficient for an anti-retroviral effect but suitable for CYP450 3A4 enzyme inhibition, and a dose normally used to boost co-administered PIs is associated with effect on the serum lipid profile. Ritonavir at this dose raises levels of LDL, total cholesterol, triglycerides, and total/HDL cholesterol ratio, as well as reduces the level of HDL cholesterol (38).

An ideal formulation of a hydrophobic drug would increase its oral bioavailability under a set of specific conditions, especially by developing lipid-based formulations. Even though solubility of the drug in lipid which is used in the preparation of formulation is a limiting factor, it must be appreciated that dose can be decreased as the bioavailability increases. Using of lipids has created more interest in commercial and academic research aspects as a key approach to develop a formulation for increasing the bioavailability of hydrophobic drugs. In general, hydrophobic drugs show low bioavailability and lower dissolution rates when administered in conventional solid formulations. It is very clear that the selection of lipid for the preparation of formulation needs to be customized for the co-administered drug to improve bioavailability. The selection of lipid not only affects the composition of formulation but also affects dynamics of the colloidal phases. This will necessitate the development of integration with *in vitro* testing procedures which consider the related physical properties and colloidal properties of lipid digestion and the association of the drugs which are co-administered along with the different colloidal phases. Apart from this, efforts are essential to identify *in vivo* models which represent the clinical scenario (39).

In the present investigation, ritonavir nanostructured lipid carriers were developed to target the lymphatic system. The development of NLCs involves selection of solid lipids and liquid lipids and a suitable surfactant that helps in stabilizing the formulation and also plays a key role in the shelf life of the formulation. Long-chain fatty acids are preferred for the transportation of drugs through lymphatic system. Lipids such as stearic acid, glyceryl monostearate, and palmitic acid consisting of more than 12 carbons were screened. Furthermore, oils such as oleic acid, castor oil, and olive oil were screened based on the amount of drug intake. Furthermore, alpha-tocopherol was used in the development of ritonavir-loaded NLCs to add the advantages of natural anti-oxidant to act against the drug-induced toxic effects. After selection of the excipients for the development of the formulation, drug-excipient compatibility studies were performed to ensure there is no effect on the chemical nature of the drug due to the excipients used in the development of the formulation. DSC and FTIR studies revealed the absence of any compatibility issues between ritonavir and the excipients used in the formulation development.

A QbD approach was followed for the development of the formulation, where all possible factors that could affect the quality of the final product were listed. The construction of the Ishikawa diagram and FMEA helped in understanding the level of criticality of the factors that could lead to the failure in the quality of the final product. The screening design selected was helpful in the determination of the most influential factors that include process parameters and material attributes on the CQAs of the product. Furthermore, optimization of the most influential factors using CCD model and the statistical analysis of the data was performed to evaluate the effect of each factor on the responses. Finally, the solutions suggested by the software for the optimized formulation were verified by comparing the experimental responses with the software predicted responses.

Dissolution studies were conducted for ritonavir pure drug suspension and optimized formulation in acidic pH conditions and pH 6.8 buffer. From the results, it is evident that drug release is more in acidic pH conditions in comparison to pH 6.8 buffer for both pure drug suspension and optimized formulation batches. However, maximum release was limited to < 20% of the total drug. The lower release of pure form of hydrophobic drugs and drug entrapped in lipid-based nanoformulations is reported in the past (12, 40). Even though the results demonstrate that there is not much release of the drug from the formulations, as the *in vitro* study can predict only to a certain extent, a preclinical study gives better understanding of the formulation behaviour in *in vivo* conditions. It is evident that in few cases especially for lipid-based formulations, it is difficult to get the *in vitro-in vivo* correlation (IVIVC) and *in vivo* studies are necessary to decide the fate of the formulation (41, 42).

The pharmacokinetic studies revealed enhanced AUC and C_{max} levels with optimized formulation (batch I) in comparison to pure drug suspension and marketed formulation. However, T_{max} and half-life were increased in pure drug suspension and marketed formulation. The elimination rate constant was higher in optimized formulation group, and mean residence time was reduced when compared to other groups. Enhancement in AUC and T_{max} can be attributed to the rapid uptake of NLCs into the lymphatic system through transcellular or paracellular access routes. As the optimized formulation is showing higher elimination rate constant, the half-life and mean residence time are reduced. Previously, Ahammed *et al.* reported twofold increment in the absorption of ritonavir using biotinylated pro-liposomes (11). Similarly, Kumar *et al.* reported that ritonavir-loaded SLNs enhanced drug absorption into plasma and tissues compared to pure drug suspension (13). In another study, Javan *et al.* reported enhanced *in vitro* activity of ritonavir-loaded SLNs; however, pharmacokinetic parameters were not reported (12). NLCs of ritonavir were prepared by Walimbe *et al.*, who exhibited an improved dissolution profile but pharmacokinetic parameters

were not reported (14). Mehta *et al.* reported 2–3-fold increment in the C_{max} and AUC of ritonavir nanosuspension in comparison to pure drug suspension. Recently, Gurumukhi *et al.* reported approximately twofold higher AUC and threefold higher C_{max} with ritonavir-loaded NLCs (43). In the current study, we observed more than 7-fold increment in the AUC and more than 10-fold higher C_{max} with the optimized formulation in comparison to pure drug suspension. Initial burst release of drug was observed during the first 1 h which can be attributed to the unentrapped portion of the drug present in the formulation. Furthermore, T_{max} was found at 2 h, whereas, in case of pure drug suspension and marketed formulation, T_{max} was found to be $\geq$ 8 h. The significant increase in AUC of drug-loaded NLCs can be attributed to the enhanced bioavailability of the drug due to the nanosized particles of NLCs which helped in improvement of the absorption. Additionally, the lipid matrix could have assisted in uptake of the NLCs through lymphatic system which would have helped in bypassing the first-pass metabolism of ritonavir. Moreover, the combination of long-chain fatty acids (stearic acid and GMS) and liquid lipids (oleic acid and alpha-tocopherol) not only enhanced the encapsulation but also sustained the effect of enzymes present in the GIT that causes the breakdown of the lipid matrix.

CONCLUSION

In the current study, nanoformulation (NLCs) was designed to encapsulate ritonavir to enhance its oral bioavailability. A natural anti-oxidant (alpha-tocopherol) was used as an excipient in the development of the formulation to encapsulate the drug. A QbD approach was followed in the development of the formulation, where screening of various excipients, designing the formulation, and optimization of the formulation were carried out. Furthermore, *in vitro* drug release profile and *in vivo* pharmacokinetic studies were conducted to understand the release profile of the drug. The novel formulation developed in the current study revealed the enhanced bioavailability of ritonavir in rodents in comparison to the pure drug and marketed formulation.

ACKNOWLEDGEMENTS

The authors are grateful to the Department of Pharmaceutics of Manipal College of Pharmaceutical Sciences (MCOPS) and Manipal Academy of Higher Education (MAHE), Manipal, Karnataka 576104, for providing the conveniences to carry out the study.

AUTHOR CONTRIBUTION

Mr. Srinivas Reddy Jitta: methodology, software, validation, formal analysis, writing—original draft and funding acquisition

Ms Navya Ajitkumar Bhaskaran: methodology, validation, formal analysis, writing—review and editing

Ms Salwa: methodology, validation, formal analysis, writing—review and editing

Dr Lalit Kumar: conceptualization, methodology, investigation, resources, writing—review and editing, supervision, and funding acquisition

FUNDING

Open access funding provided by Manipal Academy of Higher Education, Manipal. The Indian Council of Medical Research (ICMR), New Delhi, India, provided fellowship to Srinivas Reddy Jitta and Navya Ajitkumar Bhaskaran in the form of Senior Research Fellowship (SRF), and All India Council for Technical Education (AICTE), New Delhi (India), provided National Doctoral Fellowship to Salwa.

DECLARATIONS

Conflict of Interest The authors declare no competing interests.

REFERENCES

1. Deeks SG, Overbaugh J, Phillips A, Buchbinder S. HIV infection. Nat Rev Dis Primers. 2015;1:15035.
2. HIV/AIDS. Available from: https://www.who.int/news-room/fact-sheets/detail/hiv-aids. Accessed 29 Oct 2021.
3. Cihlar T, Fordyce M. Current status and prospects of HIV treatment. Curr Opin Virol. 2016;18:50–6.
4. Lv Z, Chu Y, Wang Y. HIV protease inhibitors: a review of molecular selectivity and toxicity. HIV AIDS (Auckl). 2015;7:95–104.
5. Oppong KG, Boakye-Gyasi E, Mensah KB, Obeng R, Abruquah AA, Woode E. Effectiveness of highly active antiretroviral therapy (HAART) in the adult population in the Ashanti Region of Ghana. Pharmacol Clin Pharm Res. 2021;6:53–63.
6. Xu H, Krakow S, Shi Y, Rosenberg J, Gao P. In vitro characterization of ritonavir formulations and correlation to in vivo performance in dogs. Eur J Pharm Sci. 2018;115:286–95.
7. PubChem. Ritonavir. Available from: https://pubchem.ncbi.nlm.nih.gov/compound/392622. Accessed 30 Oct 2021.
8. De Espíndola B, Beringhs AO, Sonaglio D, Stulzer HK, Silva MAS, Ferraz HG, et al. Liquisolid pellets: a pharmaceutical technology strategy to improve the dissolution rate of ritonavir. Saudi Pharm J. 2019;27:702–12.
9. Mehta C, Narayan R, Aithal G, Pandiyan S, Bhat P, Dengale S, et al. Molecular simulation driven experiment for formulation of fixed dose combination of Darunavir and Ritonavir as anti-HIV nanosuspension. J Mol Liq. 2019;293:111469.
10. Kuang C-C, Wang Y, Hu P-C, Gao F-F, Bu L, Wen X-M, Xiang QM, Song H, Li Q, Wei L, Li K. Ritonavir-induced

hepatotoxicity and ultrastructural changes of hepatocytes. Ultrastruct Pathol. 2014;38:329–34.
11. Ahammed V, Narayan R, Paul J, Nayak Y, Roy B, Shavi GV, Nayak UY. Development and *in vivo* evaluation of functionalized ritonavir proliposomes for lymphatic targeting. Life Sci. 2017;183:11–20.
12. Javan F, Vatanara A, Azadmanesh K, Nabi-Meibodi M, Shakouri M. Encapsulation of ritonavir in solid lipid nanoparticles: in-vitro anti-HIV-1 activity using lentiviral particles. J Pharm Pharmacol. 2017;69:1002–9.
13. Kumar S, Narayan R, Ahammed V, Nayak Y, Naha A, Nayak UY. Development of ritonavir solid lipid nanoparticles by Box Behnken design for intestinal lymphatic targeting. J Drug Delivery Sci Technol. 2018;44:181–9.
14. Walimbe CA, More SS, Walawalkar RU, Shah R, Ghodke D. Optimisation of nanostructured lipid carriers of Ritonavir. Inventi Rapid: NDDS. 2012;2012.
15. Anghel L, Baroiu L, Beznea A, Grigore G. The Therapeutic relevance of vitamin E. Rev Chim. 2019;70:3711–3.
16. Palipoch S, Punsawad C, Koomhin P, Suwannalert P. Hepatoprotective effect of curcumin and alpha-tocopherol against cisplatin-induced oxidative stress. BMC Complement Altern Med. 2014;14:111.
17. Caddeo C, Manca ML, Peris JE, Usach I, Diez-Sales O, Matos M, Fernàndez-Busquets X, Fadda AM, Manconi M. Tocopherol-loaded transfersomes: in vitro antioxidant activity and efficacy in skin regeneration. Int J Pharm. 2018;551:34–41.
18. Ijaz M, Akhtar N. Fatty acids based α-tocopherol loaded nanostructured lipid carrier gel: in vitro and in vivo evaluation for moisturizing and anti-aging effects. J Cosmet Dermatol. 2020;19:3067–76.
19. Graham SM, Baeten JM, Richardson BA, Bankson DD, Lavreys L, Ndinya-Achola JO, Mandaliya K, Overbaugh J, McClelland RS. Higher pre-infection vitamin E levels are associated with higher mortality in HIV-1-infected Kenyan women: a prospective study. BMC Infect Dis. 2007;7:63.
20. Beach RS, Mantero-Atienza E, Shor-Posner G, Javier JJ, Szapocznik J, Morgan R, Sauberlich HE, Cornwell PE, Eisdorfer C, Baum MK. Specific nutrient abnormalities in asymptomatic HIV-1 infection. AIDS. 1992;6:701–8.
21. Tang X, Liang Y, Liu X, Zhou S, Liu L, Zhang F, Xie C, Cai S, Wei J, Zhu Y, Hou W. PLGA-PEG Nanoparticles coated with anti-CD45RO and loaded with HDAC plus protease inhibitors activate latent HIV and inhibit viral spread. Nanoscale Res Lett. 2015;10:413.
22. Patel D, Dasgupta S, Dey S, Ramani YR, Ray S, Mazumder B. Nanostructured lipid carriers (NLC)-based gel for the topical delivery of Aceclofenac: preparation, characterization, and *in vivo* evaluation. Sci Pharm. 2012;80:749–64.
23. Cirri M, Maestrini L, Maestrelli F, Mennini N, Mura P, Ghelardini C, di Cesare Mannelli L. Design, characterization and in vivo evaluation of nanostructured lipid carriers (NLC) as a new drug delivery system for hydrochlorothiazide oral administration in pediatric therapy. Drug Deliv. 2018;25:1910–21.
24. Kasongo WA, Pardeike J, Müller RH, Walker RB. Selection and characterization of suitable lipid excipients for use in the manufacture of Didanosine-loaded solid lipid nanoparticles and nanostructured lipid carriers. J Pharm Sci. 2011;100:5185–96.
25. Mudunkotuwa IA, Minshid AA, Grassian VH. ATR-FTIR spectroscopy as a tool to probe surface adsorption on nanoparticles at the liquid–solid interface in environmentally and biologically relevant media. Analyst. 2014;139:870–81.
26. Pani NR, Nath LK, Acharya S, Bhuniya B. Application of DSC, IST, and FTIR study in the compatibility testing of Nateglinide with different pharmaceutical excipients. J Therm Anal Calorim. 2012;108:219–26.
27. Kaur P, Garg T, Rath G, Murthy RSR, Goyal AK. Development, optimization and evaluation of surfactant-based pulmonary nanolipid carrier system of paclitaxel for the management of drug resistance lung cancer using Box-Behnken design. Drug Deliv. 2016;23:1912–25.
28. Kola Srinivas NS, Verma R, Pai Kulyadi G, Kumar L. A quality by design approach on polymeric nanocarrier delivery of gefitinib: formulation, *in vitro*, and *in vivo* characterization. Int J Nanomedicine. 2016;12:15–28.
29. Bhaskaran NA, Kumar L, Reddy MS, Pai GK. An analytical "quality by design" approach in RP-HPLC method development and validation for reliable and rapid estimation of Irinotecan in an injectable formulation. Acta Pharma. 2021;71:57–79.
30. Guillot A, Couffin A-C, Sejean X, Navarro F, Limberger M, Lehr C-M. Solid phase extraction as an innovative separation method for measuring free and entrapped drug in lipid nanoparticles. Pharm Res. 2015;32:3999–4009.
31. Shibata A, McMullen E, Pham A, Belshan M, Sanford B, Zhou Y, Goede M, Date AA, Destache CJ. Polymeric nanoparticles containing combination antiretroviral drugs for HIV type 1 treatment. AIDS Res Hum Retrovir. 2013;29:746–54.
32. Gomaa E, Fathi HA, Eissa NG, Elsabahy M. Methods for preparation of nanostructured lipid carriers. Methods. Available from: https://www.sciencedirect.com/science/article/pii/S1046202321001298. Accessed 30 Oct 2021.
33. Sulkowski MS. Hepatotoxicity associated with antiretroviral therapy containing HIV-1 protease inhibitors. Semin Liver Dis. 2003;23:183–94.
34. Sulkowski MS. Drug-induced liver injury associated with antiretroviral therapy that includes HIV-1 protease inhibitors. Clin Infect Dis. 2004;38(Suppl 2):S90–7.
35. Zhong D, Lu X, Conklin BS, Lin PH, Lumsden AB, Yao Q, Chen C. HIV protease inhibitor ritonavir induces cytotoxicity of human endothelial cells. Arterioscler Thromb Vasc Biol. 2002;22:1560–6.
36. Périard D, Telenti A, Sudre P, Cheseaux JJ, Halfon P, Reymond MJ, et al. Atherogenic dyslipidemia in HIV-infected individuals treated with protease inhibitors: The Swiss HIV Cohort Study. Circulation. 1999;100:700–5.
37. Purnell JQ, Zambon A, Knopp RH, Pizzuti DJ, Achari R, Leonard JM, Locke C, Brunzell JD. Effect of ritonavir on lipids and post-heparin lipase activities in normal subjects. AIDS. 2000;14:51–7.
38. Shafran SD, Mashinter LD, Roberts SE. The effect of low-dose ritonavir monotherapy on fasting serum lipid concentrations. HIV Med. 2005;6:421–5.
39. Humberstone AJ, Charman WN. Lipid-based vehicles for the oral delivery of poorly water soluble drugs. Adv Drug Deliv Rev. 1997;25:103–28.
40. Patil PS, Dhawale SC. Development of Ritonavir loaded nanoparticles: in vitro and in vivo characterization. Asian J Pharm Clin Res. 2018;11:284–8.
41. Gordon MS, Ellis DJ, Molony B, Shah J, Teitelbaum P. In Vitro dissolution versus in vivo evaluation of four different Aspirin products. Drug Deliv Ind Pharm. 1994;20:1711–23.
42. Kollipara S, Gandhi RK. Pharmacokinetic aspects and in vitro-in vivo correlation potential for lipid-based formulations. Acta Pharm Sin B. 2014;4:333–49.
43. Gurumukhi VC, Bari SB. Development of Ritonavir-loaded nanostructured lipid carriers employing quality by design (QbD) as a tool: characterizations, permeability, and bioavailability studies. Drug Deliv Transl Res. 2021; (Ahead of printing).